Experimental study of magneto-superconductor $RuSr_2Eu_{1.5}Ce_{0.5}Cu_2O_{10-\delta}$: peculiar effect of Co doping on complex magnetism and T_c variation

2007 J. Phys.: Condens. Matter 19 026203

(http://iopscience.iop.org/0953-8984/19/2/026203)

INSTITUTE OF PHYSICS PUBLISHING JOURNAL OF PHYSICS: CONDENSED MATTER

J. Phys.: Condens. Matter **19** (2007) 026203 (14pp) doi:10.1088/0953-8984/19/2/026203

Experimental study of magneto-superconductor $RuSr_2Eu_{1.5}Ce_{0.5}Cu_2O_{10-\delta}$: peculiar effect of Co doping on complex magnetism and T_c variation

V P S Awana[1], H Kishan[1], O Eshkenazi[2], I Felner[2], Rajeev Rawat[3], V Ganesan[3] and A V Narlikar[3]

[1] National Physical Laboratory, Dr K S Kirishnan Marg, New Delhi-110012, India
[2] Racah Institute of Physics, The Hebrew University, Jerusalem, 91904, Israel
[3] UGC-DAE Consortium for Scientific Research, University Campus, Khandwa Road, Indore-452017, MP, India

E-mail: awana@mail.nplindia.ernet.in

Received 9 October 2006, in final form 30 October 2006
Published 15 December 2006
Online at stacks.iop.org/JPhysCM/19/026203

Abstract

We report structural, electrical, thermopower and magnetic properties of the $Ru_{1-x}Co_xSr_2Eu_{1.5}Ce_{0.5}Cu_2O_{10-\delta}$ ($1.0 \geqslant x \geqslant 0.0$) system. Substitution of Co at the Ru site in the $Ru_{1-x}Co_xSr_2Eu_{1.5}Ce_{0.5}Cu_2O_{10-\delta}$ system takes place iso-structurally in the tetragonal structure (space group $I4/mmm$) with full solubility ($x = 1.0$). Superconductivity (SC) exists for x up to $x = 0.075$ only and at higher Co concentrations SC is totally suppressed. The magnetic behaviour of the materials with Co up to $x = 0.2$ preserves the magnetic structure of the parent $RuSr_2Eu_{1.5}Ce_{0.5}Cu_2O_{10-\delta}$ compound. For $0.8 \geqslant x \geqslant 0.2$ an antiferromagnetic-like transition is seen at $T_N = 31$ K, which remains invariant regardless of the Co content. $CoSr_2Eu_{1.5}Ce_{0.5}Cu_2O_{10-\delta}$ ($x = 1$) seems to be an itinerant magnet, which orders magnetically at around 110 K, though for such an assertion further work is warranted. In general, the magnetization measurements as such did not reveal the complete information on the magnetic structure and hence the neutron scattering measurements are still required to resolve the complex magnetism of $Ru_{1-x}Co_xSr_2Eu_{1.5}Ce_{0.5}Cu_2O_{10-\delta}$ and even the pristine system.

1. Introduction

Genuine coexistence of superconductivity (SC) and magnetism in so-called rutheno-cuprates had been a point of debate for several years. The magneto-superconducting $RuSr_2R_{2-x}Ce_xCu_2O_{10-\delta}$ (R = Eu and Gd, Ru-1222) system was the first system in which bulk SC (T_c) in the CuO_2 planes and *weak* ferromagnetism (W-FM, T_M) in the Ru sublattice was found to coexist [1]. More recently, the second magneto-superconducting $RuSr_2RCu_2O_8$

(Ru-1212) system was discovered, which basically shows similar T_M and T_c values [2]. Both Ru-1222 and Ru-1212 phases are structurally related to the popularly known Y:123 ($YBa_2Cu_3O_{7-\delta}$) or Cu-1212, e.g. $CuBa_2YCu_2O_{7-\delta}$ phase with Cu in the charge reservoir replaced by Ru such that the Cu–O chain is replaced by a RuO_2 sheet. In the Ru-1222 structure, a three-layer fluorite-type block instead of a single oxygen-free Y layer is inserted between the two CuO_2 planes of the Cu-1212 structure [3–5]. In both systems, the SC charge carriers originate from the CuO_2 planes and the magnetic state is confined to the RuO_2 layers. The hole doping of the CuO_2 planes, which results in metallic behaviour and SC, can be optimized with appropriate variation of oxygen content or R/Ce ratio [3]. The magnetic order does not vanish when SC sets in at T_c, but remains unchanged and coexists with the SC state. Specific heat studies show a sizeable typical jump at T_c and the magnitude of the $\Delta C/T$ indicates clearly the presence of bulk SC. The specific heat anomaly is independent of the applied magnetic field [6]. Scanning tunnelling spectroscopy (STM/STS) [7], muon-spin rotation (μSR) [8] and Raman [9] experiments have demonstrated that both SC and magnetic states coexist within the same crystalline grain. SC survives (in both systems) because the Ru magnetic moments align in the basal planes, which are practically decoupled from the CuO_2 planes, so that there is no pair breaking. Though the references mentioned above are mainly for the Ru-1222 system, the same facts are in general true for the Ru-1212 system as well.

The exact nature of the magnetic structure of Ru-1222 is not yet known. However, the accumulated results indicate that the dc magnetic features of the Ru-1222 system exhibit two magnetic transitions at T_{M1} (around 80–90 K) and at T_{M2} (∼160 K). (i) For moderate applied magnetic fields ($H < 2$–3 kOe), irreversibility in the zero-field-cooled (ZFC) and field-cooled (FC) curves is observed at T_{M2}. T_{M1} is defined as the merging temperature of the ZFC and FC curves when measured at low fields ($H = 10$–20 Oe). The FC curves all show ferromagnetic-like shape, whereas the dc ZFC curves (as well as the ac susceptibility plots) show a well distinguished peak around T_{M1}. For higher external fields ($H > 5$ kOe), both ZFC and FC curves collapse to a single ferromagnetic-like behaviour. It is thus proposed that at T_{M1} weak ferromagnetism (W-FM) sets in, which originates from canting of the Ru moments. This canting is a result of the tilting of the RuO_6 octahedra away from the crystallographic c axis [10]. In the $M(H)$ curves, relatively wide FM hysteresis loops are opened at low temperatures (the coercive field—$H_c \sim 450$–500 Oe at 5 K), which become narrow as the temperature increases and practically disappears around 60–70 K. The FM-like hysteresis loops obtained at low temperatures are also consistent with W-FM order in this region. (ii) Above T_{M1}, a *second* small peak is observed around 120 K in both dc and ac susceptibility curves and small canted AFM-like hysteresis loops are observed [11]. The $H_c(T)$ curves show a peak with a maximum around 120 K ($H_c \sim 150$ Oe) and become zero at T_{M2} [12]. In the stoichiometric $RuEuCeSr_2Cu_2O_{10}$ ($x = 1$) compound none of these peaks are observed. In this region, at high H, the Ru moments are realigned through a spin–flip process, to form the AFM-like shape hysteresis loops.

One of the disputed questions is the *origin* of the higher magnetic transition at T_{M2}, in Ru-1222 materials, whether is it intrinsic or not [13]. The qualitative results are compatible with two alternative scenarios. Our preferred scenario (A) assumes that this is an intrinsic bulk property, and that the two magnetic transitions are connected to each other. The second transition appears only for samples with less Ce^{4+} ($x < 1$) where the reduction of Ce content is compensated for by depletion of oxygen, which is not homogeneous throughout the whole material. Ru^{5+} ions are surrounded by less oxygen as first neighbours and hence reduced to Ru^{4+}. The Ru^{4+}–Ru^{4+} exchange interactions are stronger than the Ru^{5+}–Ru^{5+} ones and hence have higher magnetic transition. A small fraction of nano-domain species inside the crystal grains of Ru-1222 in which the Ru^{4+} concentration is high becomes AFM ordered at

T_{M2} (∼160 K). This scenario is consistent with a quantitative XANES study which revealed an average Ru valence value of 4.74 for as-prepared Ru-1222 material [14]. Qualitatively speaking, the Ru-1222 system is quite similar to the Ru-1212 one, in which NMR experiments suggest that the Ru ions may be in a mixed valence state with 40% Ru^{4+} ($S = 1$) and 60% Ru^{5+} [15]. An alternative scenario assumes that in Ru-1222 (except for $x = 1$), due to oxygen depletion, the reduction to Ru^{4+} leads to the presence of an extra impurity phase (about 5%, undetected by XRD) of Sr–Cu–Ru–O_3 phase, which orders at T_{M2}. The exact composition of this phase, in which Cu atoms distribute themselves inhomogeneously at the Ru or Sr sites, is sample dependent, which is determined by the Ce and/or oxygen concentration as well as by the preparation conditions. This extra phase also shows (a) the typical increase in H_c around 120 K [13]. It is worth noting that we stress the origins of T_{M1} (around 80–90 K) and T_{M2} (∼160 K) in Ru-1222 due to the fact that in many works this important reproducible aspect is ignored. Both T_{M1} and T_{M2} should be taken into account with regard to the complex magnetism of Ru-1222. Besides T_{M1} and T_{M2}, also important is the *second* small peak above T_{M1}, i.e., T_{M21} observed at around 120 K in both dc and ac susceptibility curves.

To investigate the relationship between SC and magnetism in Ru-1222, we have attempted to replace Cu^{2+} by non-magnetic Zn^{2+} ions [7]. Similar to all other Zn doped high T_c materials, tiny amounts of Zn are sufficient to suppress the SC state ($T_c = 38$ K) and the material with 1.25 at.% of Zn is not SC down to 4.2 K. On the other hand, the magnetic state of the Ru sublattice is not significantly affected by the presence or absence of the SC state. This proves that the two states are practically decoupled [12]. We also studied the effect of *non-magnetic* Sn^{4+} and Al^{3+} ion substitution for Ru^{5+}, on both SC and magnetic states of Ru-1222. It appears that about 7 at.% of Al ions are needed to destroy the SC state. Since such substitutions dilute the magnetic RuO_2 layers, it was shown that Al substitution (up to 10%) shifts only T_{M2} to lower temperatures, but does not alter much T_{M1}. On the other hand, the substitution of 5% of Sn affects dramatically both T_{M1} and T_{M2}, and shifts them to lower temperatures [16].

Here we present the substitution effect of *magnetic* Co ions for Ru, on both SC and magnetic properties of the Ru-1222 system. Ru-site Co substitution could be a right choice, because both Ru-1222 and $CoSr_2Eu_{1.5}Ce_{0.5}Cu_2O_{10-\delta}$ (Co-1222) [17] are iso-structural to each other and therefore this permits a full substitution of Co for Ru. Note that in the $Ru_{1-x}Co_x$-1212 system Co substitution is reported up to 20% only [18]. It is shown that that both the SC properties and the magnetic behaviour can be divided into three regimes. Our resistivity and thermoelectric power (TEP) measurements indicate clearly that in the mixed $Ru_{1-x}Co_xSr_2Eu_{1.5}Ce_{0.5}Cu_2O_{10-\delta}$ system, SC decreases with Co and the full SC state (zero resistance) is obtained only for $x < 0.05$. For $0.1 \geqslant x \geqslant 0.05$, only the onset of the SC state is observed, whereas for higher Co concentrations ($x \geqslant 0.1$) the materials are not SC; in this sense this system behaves similarly to the non-magnetic Al doped Ru-1222 as described above. Interestingly enough, the complicated magnetic features and the two magnetic transitions of Ru-1222 described above persist up to $x = 0.2$ and both T_{M1} and T_{M2} do not alter much with x. For higher x concentration up to $x = 0.8$, the materials are AFM ordered with a similar $T_N \sim 31$–33 K value. The pure Co-1222 material probably orders magnetically below 140–150 K and its magnetic behaviour is discussed.

2. Experimental details

The $Ru_{1-x}Co_xSr_2Eu_{1.5}Ce_{0.5}Cu_2O_{10-\delta}$ ($1.0 \geqslant x \geqslant 0.0$) samples were synthesized through a solid-state reaction route from stoichiometric amounts of RuO_2, SrO_2, Eu_2O_3, CeO_2, CuO and Co_2O_3; nearly the same heat treatments are followed as for $Ru_{1-x}Mo_xSr_2Eu_{1.5}Ce_{0.5}Cu_2O_{10-\delta}$

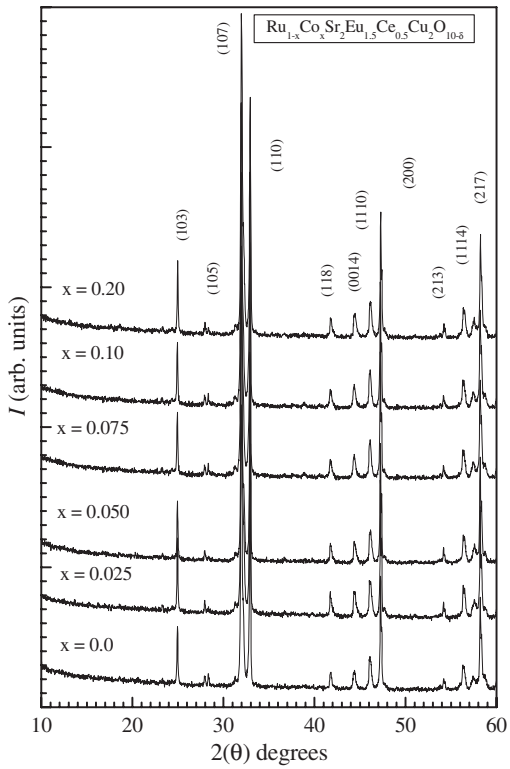

Figure 1. XRD patterns of the $Ru_{1-x}Co_xSr_2Eu_{1.5}Ce_{0.5}Cu_2O_{10-\delta}$ ($0.2 \geqslant x \geqslant 0.0$) system.

(preceding article). X-ray diffraction (XRD) measurements confirmed the purity of the compounds. Within the instrumental accuracy, all the $Ru_{1-x}Co_xSr_2Eu_{1.5}Ce_{0.5}Cu_2O_{10}$ samples have the same tetragonal structure (space group $I4/mmm$). The dc magnetic measurements were performed in a commercial (Quantum Design) superconducting quantum interference device (SQUID) magnetometer. The ac susceptibility was measured at $H_{dc} = 0$ by a home made probe inserted in the SQUID, with an excitation frequency of 733 Hz and amplitude of 120 mOe. Resistivity measurements were carried out by the conventional four-probe method. Thermoelectric power measurements were carried out by the dc differential technique over a temperature range of 5–300 K, using a home made set-up. A temperature gradient of ∼1 K was maintained throughout the TEP measurements.

3. Results and discussion

3.1. X-ray diffraction

Figure 1 depicts the x-ray diffraction (XRD) patterns for $Ru_{1-x}Co_xSr_2Eu_{1.5}Ce_{0.5}Cu_2O_{10-\delta}$ ($0.2 \geqslant x \geqslant 0.0$). As mentioned above, the Co substitution for Ru in Ru-1212 is successful within the same structural phase only until 20% [18]. In fact, full substitution of Co at the Ru site in Ru-1212 results in a change of space group from $P4/mmm$ to $Ima2$ due to doubling of the unit cells arising from the superstructures [19]. In the case of Ru-1222, the basic unit cell is already doubled, having space group $I4/mmm$, and hence Co substitution takes place iso-structurally within the same group with full solubility [17]. It is evident from

this figure that all samples crystallize in a single phase with tetragonal structure (space group $I4/mmm$). Respective Miller indices are shown in the figure. It is to be noted that a few unidentified lines are also seen in the x-ray diffraction pattern, namely at 2θ of nearly 28° and 58°. Though we could not identify them, they are not from Ru-1212, $SrRuO_3$ or another possible culprit, $RuSr_2EuO_6$. Most probably they arise from the super-structures of the tilted RuO_6 octahedra of the system [10, 20]. Due to the similarity in the ionic radii of Ru^{5+} (0.71 Å) and Co^{3+} in the low spin mode (0.69 Å), the lattice parameters of both end compounds are quite similar: for $RuEu_{1.5}Ce_{0.5}Sr_2Cu_2O_{10-\delta}$ $a = 3.827(1)$ Å and $c = 28.48(2)$ Å and for $CoEu_{1.5}Ce_{0.5}Sr_2Cu_2O_{10-\delta}$ $a = 3.829(1)$ Å and $c = 28.47(2)$ Å. This implies that (within the instrumental accuracy) the lattice parameters of all mixed materials are independent of the Co content. We can safely conclude at this point that, unlike the case for Ru-1212, in the Ru-1222 system the substitution of Co at the Ru site takes place iso-structurally in a single phase within the accuracy of x-ray limits.

3.2. The superconducting state in $Ru_{1-x}Co_xSr_2Eu_{1.5}Ce_{0.5}Cu_2O_{10-\delta}$

All experiments including transport and magnetization measurements performed on the $Ru_{1-x}Co_xSr_2Eu_{1.5}Ce_{0.5}Cu_2O_{10-\delta}$ system indicate coexistence of SC and magnetism for samples with Ru content ($x < 0.1$), while the materials with higher Co concentration are magnetically ordered only. This will be shown in the next sections. In this respect this system behaves very differently from the $Ru_{1-x}Mo_xSr_2Eu_{1.5}Ce_{0.5}Cu_2O_{10-\delta}$ system [21], where superconductivity is observed until $x = 0.60$.

The absolute thermopower $S(T)$ curves for $Ru_{1-x}Co_xSr_2Eu_{1.5}Ce_{0.5}Cu_2O_{10-\delta}$ up to $x = 0.2$ are shown in figure 2. The positive $S(T)$ values over the entire range confirm that the carriers are holes. The $S(T)$ curves show features at the onset of the SC defined as T_c. For $x = 0$ and 0.025 the $S(T)$ curves exhibit a break in the slope at $T_c = 37.5$ and 29 K respectively which are in good agreement with resistivity measurements presented in inset of figure 2. The drop to zero at 27 and 20.5 K respectively is relatively broad, suggesting that the sample doping may be inhomogeneous, leading to $S(T) = 0$ at the percolation transition, that is complete at 27 and 20.5 K respectively. This general behaviour is reminiscent of an under-doped high T_c cuprate system and is in general agreement with other reports on Ru-1222 [22–24]. For $x = 0.05$ and 0.075 we obtain $T_c = 22$ and 20 K but no percolation transition is observed. The materials with higher Co content are not SC. The $S(T)$ curves in figure 2 are quite linear up to 90–100 K, indicating a very metallic-like behaviour, after which they begin to flatten. There are no clear features at the magnetic transitions as determined by dc and ac susceptibility measurements to be discussed in the next sections.

Resistivity versus temperature $\rho(T)$ measurements are performed at varying temperatures. Generally speaking the materials are divided into three groups.

(i) The materials with $x = 0$ and $x = 0.025$ exhibit a slight semiconducting behaviour down to 200 K and metallic character with a small positive slope below 200 K. Since the curves of the field dependence of $\rho(T)$ for the pure $x = 0$ material have already been shown in the past [22–25] and in a very recent report in [26], we present in figure 3 the data obtained for the $x = 0.025$ material only. The T_c and $T_c^{\rho=0}$ (at $H = 0$) for both materials are similar to the values deduced from TEP studies (figure 2): e.g. for $x = 0.025$, $T_c = 30$ K and $T_c^{\rho=0} = 19$ K. This sample exhibits a slight semiconducting behaviour above T_c. It is readily observed that the broad SC transition occurs via two stages. The onset at $T_c = 30$ K at which the grains become SC is not affected by H and little difference in T_c is observed between 0 and 5 T. However, the step-like transition at 24 K (at zero field), which is due to weak Josephson inter-grain coupling, does not change much up to 1 T, but is affected

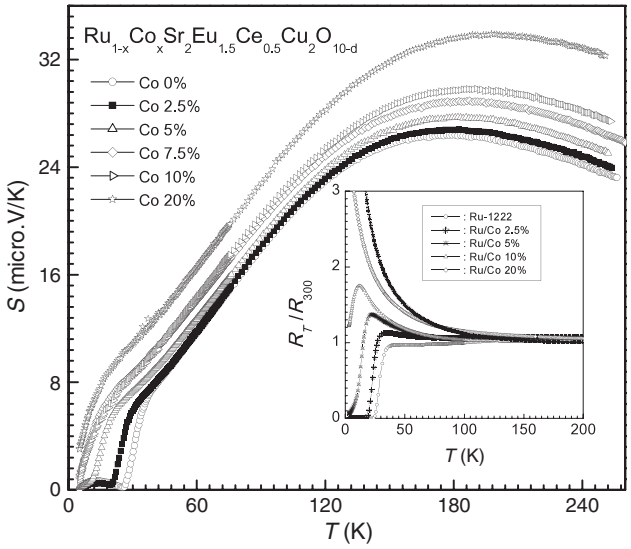

Figure 2. Thermopower plots of the $Ru_{1-x}Co_xSr_2Eu_{1.5}Ce_{0.5}Cu_2O_{10-\delta}$ ($0.2 \geqslant x \geqslant 0.0$) system; the inset shows the normalized resistivity behaviour of the same.

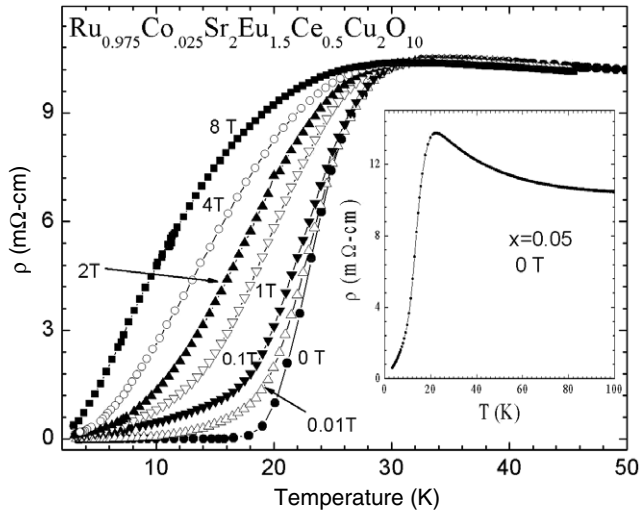

Figure 3. Plots of resistivity under various magnetic fields for the $Ru_{0.975}Co_{0.025}Sr_2Eu_{1.5}Ce_{0.5}Cu_2O_{10-\delta}$ system; the inset shows the onset of superconductivity for $x = 0.05$.

dramatically at higher applied fields. This is typical for granular superconductors with weak inter-grain coupling in which the resistivity is governed mainly by the weak link properties. The zero resistance temperature ($T_c^{\rho=0}$) decreases rapidly at low fields and only slowly at high fields. Figure 3 shows that $T_c^{\rho=0}$ decreases to ∼6 K at $H = 4$ T but does not reach zero (down to 2 K) under $H = 8$ T. The decrement rate of $T_c^{\rho=0}$ is nearly 3.2 K T^{-1} (2.5 K T^{-1} for $x = 0$), though it is not linear as is the case for any type II superconductor.

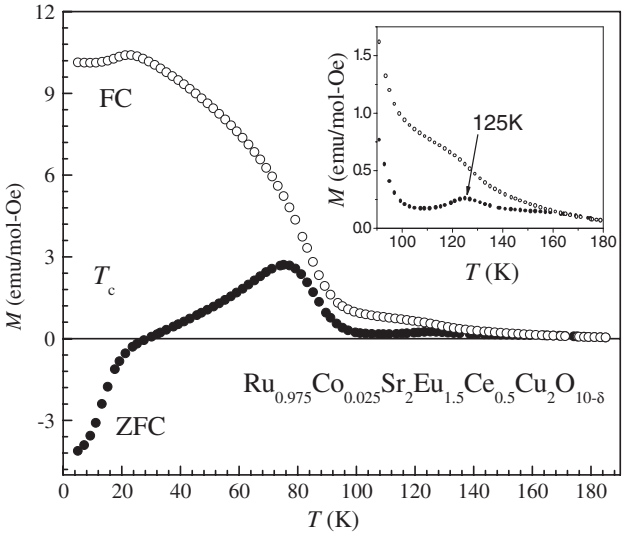

Figure 4. ZFC and FC curves at 4 Oe for $Ru_{0.975}Co_{0.025}Sr_2Eu_{1.5}Ce_{0.5}Cu_2O_{10-\delta}$; note the second peak in the extended scale of the inset.

(ii) Samples with $x = 0.05$ and $x = 0.075$. Figure 3 (inset) depicts the $\rho(T)$ plot at $H = 0$ for the $x = 0.05$ compound. Here again, the curve exhibits a sharp drop at the onset $T_c = 20$ K (10 K for $x = 0.075$) but does not become zero down to 2 K. The normal state resistivity behaviour is purely semiconducting with no regions of metallic segments in between. Unlike the case of group (i), T_c decreases monotonically with the applied field, and no onset of SC is obtained for H higher than 4 T. This indicates the possible SC/semi-conducting/SC stacking behaviour, which is the general trend that exists for most highly under-doped/disordered HTSC compounds.

(iii) SC is totally suppressed for all samples with $x \geqslant 0.1$ which are highly semiconducting down to 2 K. Please see the $\rho(T)$ curve for $x = 0.10$ in figure 6 (inset). Interestingly, a small amount of magneto-resistance under 8 T (not shown) is observed for $x = 0.1$ and $x = 0.2$, which is probably the result of a magnetic phase separation occasionally found in the ruthenates when changing the oxygen content and/or the disorder in RuO_6 octahedra [25, 27, 28].

3.3. The magnetic state in $Ru_{1-x}Co_xSr_2Eu_{1.5}Ce_{0.5}Cu_2O_{10-\delta}$

The magnetic properties of the $Ru_{1-x}Co_xSr_2Eu_{1.5}Ce_{0.5}Cu_2O_{10-\delta}$ can also be divided into three regions.

(i) $0.2 \geqslant x \geqslant 0$. The magnetic behaviour of all samples in this region is quite similar; it means that the two magnetic transitions discussed above are present. Coexistence of SC and magnetism appears for samples with high Ru content ($x < 0.075$), while the materials with higher Co concentration are magnetically ordered only. Since the magnetization plots for the pure $x = 0$ material have been presented and discussed in [26], figures 4 and 5 exhibit the dc ZFC and FC plots (measured at 4 Oe) and the real ac susceptibility curve for the $x = 0.025$ material, which behaves similarly to the $x = 0$ sample. The negative signals in both figures represent clearly the SC state of this material. On the other hand

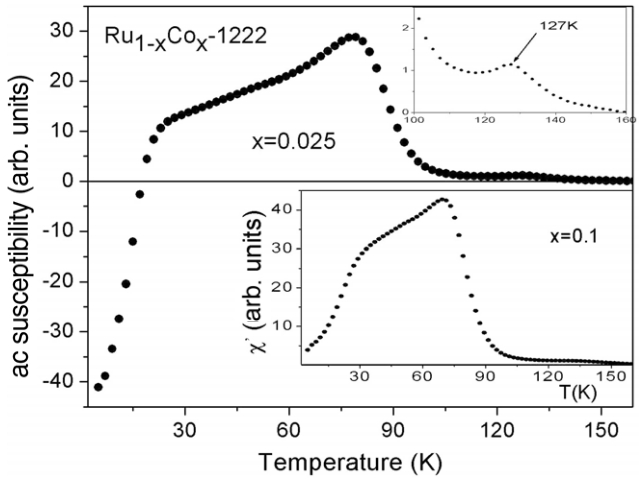

Figure 5. Real ac susceptibility plots for $Ru_{0.975}Co_{0.025}Sr_2Eu_{1.5}Ce_{0.5}Cu_2O_{10-\delta}$ and $Ru_{0.90}Co_{0.10}Sr_2Eu_{1.5}Ce_{0.5}Cu_2O_{10-\delta}$ materials.

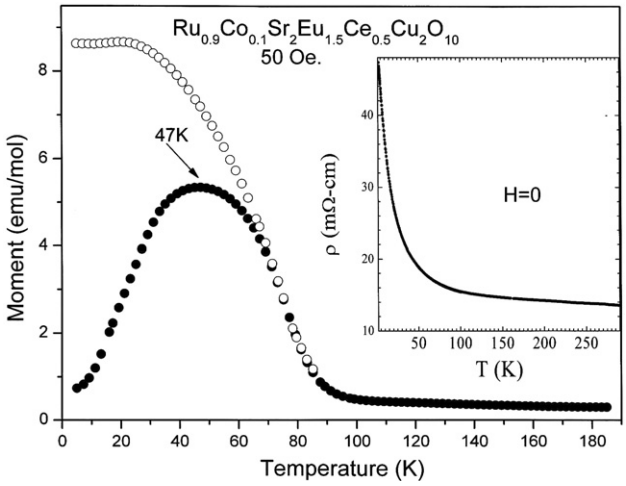

Figure 6. ZFC and FC branches measured at 4 Oe and the resistivity (inset) for the $Ru_{0.90}Co_{0.10}Sr_2Eu_{1.5}Ce_{0.5}Cu_2O_{10-\delta}$ sample.

the positive values of the ZFC as well as the ac curves for $x = 0.1$ and $x = 0.2$ samples (figures 6, 7) indicate that the samples are not SC. This is in perfect agreement with the TEP and resistivity data presented in figures 2 and 3 respectively. The main magnetic peak position is shifted to lower temperatures with increasing x: $T_{M1} = 89$ K for $x = 0$ and 35 K for $x = 0.2$. On the other hand, T_{M2} for all samples defined by the saturation moment M_{sat} (described below) does not alter much ($T_{M2} \sim 150$–160 K). The clear second peak around 125 K (T_{M21}) for $x = 0.025$ remains practically unchanged up to $x = 0.1$. (For $x = 0.2$ the second peak is visible but smeared.) The variations of T_{M1} and T_{M21}, as well as the T_c values of the SC materials as a function of Co concentration, are summarized in figure 8. Note the different assignment of the $x = 0$ and 0.025 samples in which zero resistance and $S(T)$ values were observed (figures 2 and 3).

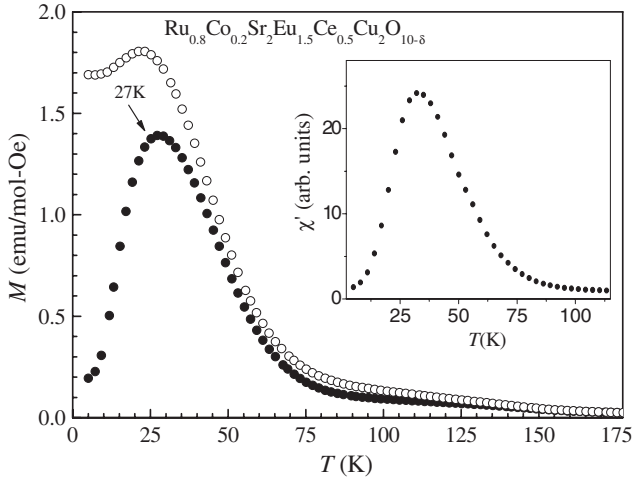

Figure 7. ZFC and FC branches measured at 4 Oe and the ac susceptibility (inset) for the $Ru_{0.80}Co_{0.20}Sr_2Eu_{1.5}Ce_{0.5}Cu_2O_{10-\delta}$ sample.

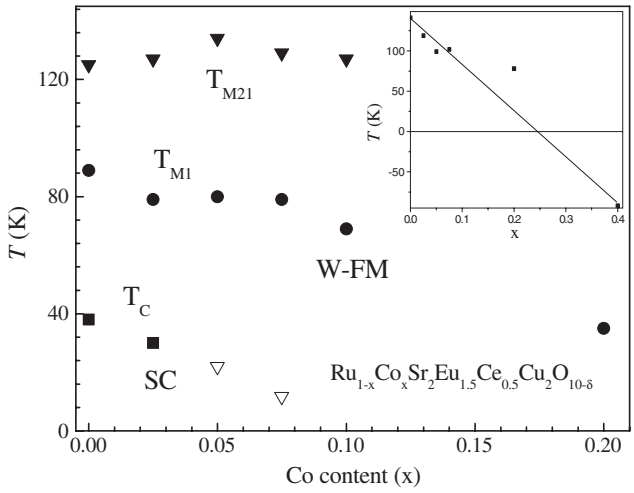

Figure 8. Phase diagram of the SC and the two magnetic states as functions of x for $Ru_{1-x}Co_xSr_2Eu_{1.5}Ce_{0.5}Cu_2O_{10-\delta}$; the samples with zero TEP and resistivity are marked in full symbols. The inset shows the variation of Curie–Weiss temperatures with x.

The isothermal $M(H)$ for all samples has been measured at various temperatures. The $M(H)$ curves are strongly dependent on the field (up to 2–3 kOe), until a common slope is reached. At low applied fields, the $M(H)$ curve exhibits a typical ferromagnetic-like hysteresis loop similar to that reported in [1, 3, 12, 16, 25, 26] and discussed in [26] for pristine $RuSr_2Eu_{1.5}Ce_{0.5}Cu_2O_{10-\delta}$ magneto-superconductor. At higher fields, an apparent tendency toward saturation is obtained, without reaching full saturation even with 5 T field at 5 K. The $M(H)$ curves can be described as $M(H) = M_{sat} + \chi H$, where M_{sat} corresponds to the W-FM contribution of the Ru sublattice, and χH is the linear paramagnetic contribution of Eu, Co and Cu. A gradual linear decrease (at 5 K) of M_{sat} with x is obtained (from $0.62(1)\mu_B$ for $x = 0$ to $0.11(1)\mu_B$ for $x = 0.2$), indicating the

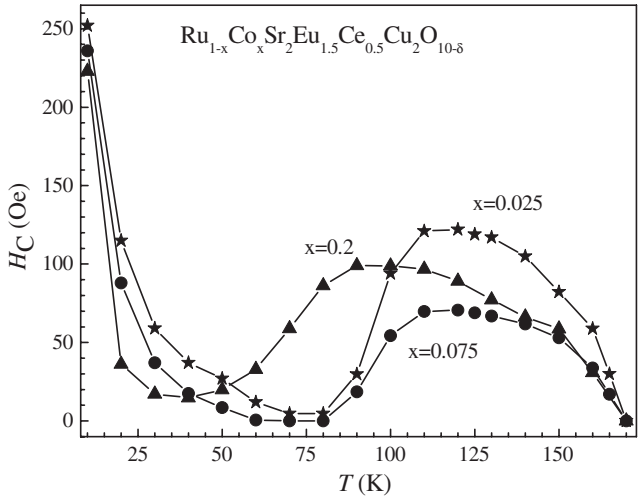

Figure 9. The temperature dependence of the coercive field for various materials.

dilution of the magnetic Ru^{5+} ions by Co ions. The temperature dependence of M_{sat} for all materials studied shows an FM type behaviour and becomes zero at T_{M2}(Ru) = 150–160 K(2), regardless of their Co concentration.

The more interesting effects to be seen are exhibited in figure 9. The relatively wide FM hysteresis loops opened at low temperatures ($H_c \sim$ 400–450 Oe at 5 K) become narrow as the temperature increases and practically disappear at 30 and 60 K for the high Co concentration, respectively. However, at higher temperatures, small canted AFM-like hysteresis loops are reopened for all samples [11, 29] and the $H_c(T)$ curves show a peak with a maximum at 100 and 125 K respectively, and become zero at T_{M2}. The shift in the minimum position of H_c for the $x = 0.2$ material is consistent with the low T_{M1} position shown in figure 7.

Without a detailed magnetic structure from neutron diffraction studies, it is difficult to comment on the exact nature of the magnetic behaviour in this region. The small second peak in the magnetization curves and the rise in H_c are not straightforward. However, our conclusions are as follows. (i) We assume that the two phenomena are connected to each other and have the same origin. (ii) Figure 9 shows that the SC material ($x = 0.025$) and the non-SC one ($x = 0.2$) have basically the same T_{M2}(Ru) and a similar H_c trend. (iii) The magnetic structure of all samples is practically the same regardless of their Co content.

Above T_{M2}, the $\chi(T)$ curves (measured at 10 kOe) for $x = 0$–0.075 and 0.2 have the typical paramagnetic shape and adhere closely to the Curie–Weiss (CW) law: $\chi(T) = \chi_0 + C/(T-\theta)$, where χ_0 is the temperature independent part of χ, C is the Curie constant and θ is the CW temperature. Unexpectedly, the sample with $x = 0.1$ does not follow the CW behaviour. Since the Eu^{3+}, Cu^{2+} and Co ions all contribute to C and due to uncertainty in the Ru ion valence, the net Ru contributions to $\chi(T)$ were not calculated. On the other hand, the θ values decrease with x, $\theta = 141$ K for $x = 0$ and 78 K for $x = 0.2$ (figure 8 inset), in full agreement with the shift of T_{M1} (figure 8, main frame).

(ii) $0.8 \geqslant x \geqslant 0.4$. Figure 10 shows that the magnetic behaviour of the samples with high Co concentration is quite different. The temperature dependences of the magnetic susceptibility in the ZFC and FC processes for $x = 0.4$ and 0.8 are shown in figure 10.

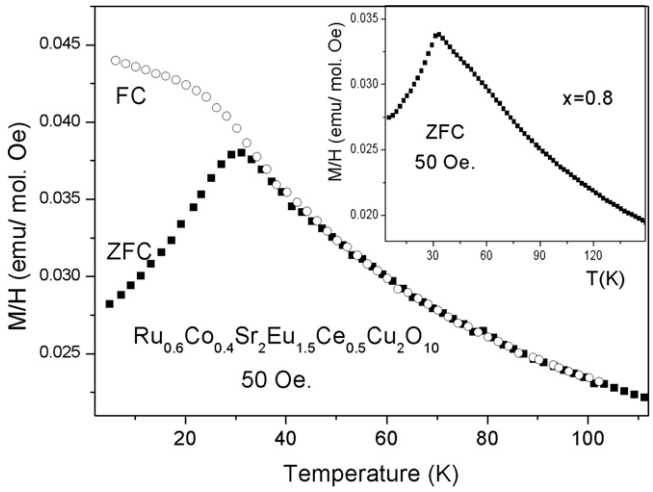

Figure 10. ZFC and FC branches of dc magnetization for $Ru_{0.60}Co_{0.40}Sr_2Eu_{1.5}Ce_{0.5}Cu_2O_{10-\delta}$ and $Ru_{0.20}Co_{0.80}Sr_2Eu_{1.5}Ce_{0.5}Cu_2O_{10-\delta}$ compounds.

A distinct peak at 31 K is observed in the ZFC branches and no other anomalies were observed at higher temperatures. Therefore, we may assume that all three samples studied ($x = 0.4$, 0.6 and 0.8) are AFM ordered with the same T_N value. In the FC process the external field causes the spins to cant slightly out of their original direction. This canting abruptly aligns a component of the moment with the direction of the field and the FC branch is obtained. The $M(H)$ curves at 5 K are linear up to 5 T and the negative paramagnetic θ value obtained (−92 K for $x = 0.4$, figure 8 inset) supports this determination. The $x = 0.6$ and 0.8 materials do not follow the CW behaviour.

Since the presumed T_N does not change with Co, the question raised is which ions are responsible for this magnetic anomaly. It is possible that, similar to the case of Fe in $CoSr_2Eu_{1.5}Ce_{0.5}Cu_2O_{10-\delta}$ [30], the Ru–Co sublattice is not magnetically ordered, and that the magnetic anomalies in figure 10 are related to the Cu sites. Also, it was observed earlier that for fully Co substituted samples a small fraction of the Co ions also reside in the CuO_2 planes [17]. The relatively low $T_N = 31$ K in these materials is a result of some frustration of the Cu moments by the presence of Co in the Cu sites. It is worth mentioning here that the explanation provided above is purely an assumption, and neutron scattering measurements at low temperatures are warranted to understand the complex magnetic structure of these samples.

(iii) $CoSr_2Eu_{1.5}Ce_{0.5}Cu_2O_{10-\delta}$. The temperature dependence of the ZFC curve measured at 1 kOe for the $x = 1$ material is shown in figure 11. No difference between the ZFC and FC branches is observed. Here, again, the isothermal $M(H)$ curve measured at 5 K is linear up to 5 T and the high temperature range of the M/H curve does follow the CW law. The nature of the shallow peak around 110 K does not shed light on the magnetic behaviour of this compound.

Mössbauer spectroscopy studies (MS) of dilute ^{57}Fe probes have proved to be a powerful tool in the determination of the magnetic nature of the probe's site location. When the host ions become magnetically ordered, they produce an exchange field on the neighbouring Fe ions. The ^{57}Fe nuclei experience magnetic hyperfine fields, leading to sextets in the observed MS spectra. For example, in Ru-1222, the dilute Fe successfully follows the Ru magnetization and

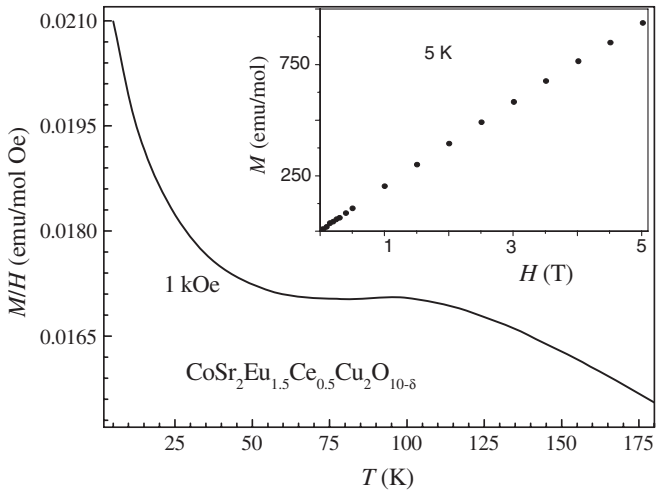

Figure 11. ZFC and FC curves and the linear $M(H)$ plot at 5 K (inset) for the $CoSr_2Eu_{1.5}Ce_{0.5}Cu_2O_{10-\delta}$ sample.

well defined magnetic hyperfine fields are visible in the MS spectra up to T_{M2} [1]. In our recent publication [30], using the MS technique, we have shown that Fe ions in Ru-1222 are found to occupy predominantly the Ru (Co) sites, and the rest reside in the CuO_2 planes.

MS on a Co-1222 sample containing ∼1% ^{57}Fe was performed at 300 and 90 K using a conventional constant acceleration drive and 50 mCi ^{57}Co:Rh sources (spectra not shown). The experimental spectra were analysed in terms of two sub-spectra, by a least square fit procedure. The main information obtained at 300 K is the presence of two quadrupole doublets corresponding to inequivalent Fe sites, which are immediately identified by their hyperfine parameters. Since the crystal structures of Ru(Co)-1222 and YBCO are closely related, we assign here the doublets according to the Fe-site assignment in YBCO [31]. It is well accepted that in YBCO the Fe ions are found to occupy predominantly the Cu(1) site, which is equivalent to the Co site in Co-1222. A similar behaviour is observed here. The dominant doublet (69%), isomer shift (IS) 0.132 mm s^{-1} (relative to Fe metal) and quadrupole splitting $(1/2e^2Qq) = 1.44$ mm s^{-1}, corresponds to the Co site and the minor one (31%), IS $= 0.171$ mm s^{-1} and $1/2e^2Qq = 0.62$ mm s^{-1}, corresponds to the Cu sites. At 90 K (below the flat peak in figure 11), the major doublet is broadened, and our analysis indicates clearly the presence of small magnetic hyperfine fields (10.9 kOe) at the Co site. The doublet belongs to the Cu and is not affected by reducing the temperature. This may indicate that the Co sublattice orders magnetically at 110 K. We speculate that the Co magnetic order has an itinerant nature. The intriguing question arises as to why here the Co and not the Cu sublattice is magnetic. More experiments are being carried on to clarify this point. Here again we would like to mention that to understand the complex magnetism of $Ru_{1-x}Co_xSr_2Eu_{1.5}Ce_{0.5}Cu_2O_{10-\delta}$ system neutron scattering experiments are warranted.

4. Summary

Each of the two SC and magnetic states in $Ru_{1-x}Co_xSr_2Eu_{1.5}Ce_{0.5}Cu_2O_{10-\delta}$ could be divided into three parts. The onset of the SC transition decreases with x up to $x = 0.075$, but only the samples with $x = 0$ and 0.025 show zero TEP and resistivity at low temperatures (figures 2, 3).

For $x > 0.075$ SC is totally suppressed and the materials exhibit a semiconducting behaviour. Hole density in the CuO_2 planes, or deviation of the formal valence from Cu^{2+}, is the primary parameter, which governs T_C in most HTSC compounds. It seems SC emerges only in a narrow window of the carrier concentration. Also, Co in the doped Ru-1222 may reside partially in both Ru and Cu sites in 1222 systems [17], thus not only it modifies the hole density and the optimum charge carriers of the CuO_2 planes but creates disorder in CuO_2 planes and therefore for higher concentration SC is suppressed. Both SC (which is confined to the Cu–O layers) and magnetic states of the Ru(Co) sublattice, which coexist below T_c, appear practically decoupled from each other. The detailed magnetic structure is not known yet.

For higher Co concentration up to $x = 0.8$, the complicated magnetic structure does not exist. Rather a clear AFM transition at $T_N = 31$ K (figure 10) is observed regardless of the Co concentration. Thus it is assumed that this magnetic order is due to the Cu ions in the CuO_2 planes. The relative T_N of this system, as compared to other M-1222 compounds [32], is probably a result of frustration of the Cu moments. In the case of the $CoSr_2Eu_{1.5}Ce_{0.5}Cu_2O_{10-\delta}$ system, the susceptibility curve does not permit any easy determination of whether this compound is magnetically ordered or not. However, MS measurements indicate that the Co sublattice is probably magnetically ordered at 110 K. More experiments are needed to clarify its nature.

Acknowledgments

This research is supported by the Indo-Israel collaborative DST (Department of Science and Technology, India) and MST (Ministry of Science and Technology, Israel) project. The research in Israel is also partially funded by Israel Science Foundation (ISF, 2004 grant number 618/04), and by the Klachky Foundation for Superconductivity. Authors from the NPL appreciate the interest and advice of Professor Vikram Kumar (Director) in the present work.

References

[1] Felner I, Asaf U, Levi Y and Millo O 1997 *Phys. Rev.* B **55** R3374
[2] Bernhard C, Tallon J L, Niedermayer Ch, Blasius Th, Golnik A, Brücher E, Kremer R K, Noakes D R, Stronack C E and Asnaldo E J 1999 *Phys. Rev.* B **59** 14099
[3] Awana V P S 2005 Magneto-superconductivity of rutheno-cuprates *Magnetic Materials* ed A V Narlikar (Berlin: Springer) pp 531–72 (review chapter)
[4] Bauernfeind L, Widder W and Braun H F 1995 *Physica* C **254** 151
[5] Sakai N, Maeda T, Yamauchi H and Tanaka S 1993 *Physica* C **212** 75
[6] Chen X H, Sun Z, Wang K Q, Li S Y, Xiong Y M, Yu M and Cao I Z 2001 *Phys. Rev.* B **63** 064506
[7] Felner I, Asaf U, Levi Y and Millo O 2000 *Physica* C **334** 141
[8] Shengelaya A, Khasanov R, Eshchenko D G, Felner I, Asaf U, Keller H and Muller K H 2004 *Phys. Rev.* B **69** 024517
[9] Williams G V M and Ryan M 2001 *Phys. Rev.* B **64** 094515
[10] Knee C S, Rainford B D and Weller M T 2000 *J. Mater. Commun.* **10** 2445
[11] Felner I, Awana V P S and Takayama-Muromachi E 2003 *Phys. Rev.* B **68** 094508
[12] Felner I, Galstyan E, Awana V P S and Takayama-Muromachi E 2004 *Physica* C **408–410** 161
[13] Felner I, Galstyan E and Nowik I 2005 *Phys. Rev.* B **71** 064510
[14] Awana V P S, Karppinen M, Yamauchi H, Matvejeff M, Liu R S and Yang L-Y 2003 *J. Low Temp. Phys.* **131** 1211
[15] Tokunga Y, Kotegawa H, Ishida K, Kitaoka K, Takagiwa H and Akimitsu J 2001 *Phys. Rev. Lett.* **86** 5767
[16] Felner I, Galstyan E, Herber R H and Nowik I 2004 *Phys. Rev.* B **70** 094504
[17] Awana V P S, Gupta A, Kishan H, Malik S K, Yelon W B, Lindén J, Karppinen M, Yamauchi H and Kundaliya D C 2004 *J. Appl. Phys.* **95** 6690
[18] Yang L T, Liang J K, Liu Q L, Song G B, Liu F S, Luo J and Rao G H 2004 *Physica* C **403** 177

[19] Awana V P S, Malik S K, Karppinen M, Yamauchi H and Yelon W B 2002 *Physica* C **378–381** 153
[20] Yokosawa T, Awana V P S, Kimoto K, Takayama-Muromachi E, Karppinen M, Yamauchi H and Matsui Y 2004 *Ultramicroscopy* **98** 283–95
[21] Awana V P S, Lal R, Kishan H, Narlikar A V, Peurla M and Laiho R 2006 *Phys. Rev.* B **73** 014517
[22] Zivkovic I, Hirai Y, Frazer B H, Prester M, Drobac D, Ariosa D, Berger H, Pavuna D, Margaritondo G, Felner I and Onillion M 2001 *Phys. Rev.* B **65** 144420
[23] Henning B D, Rathnayaka K D D, Naugle D G and Felner I 2002 *Physica* C **370** 253
[24] Felner I, Galstyan E, Lorenz B, Cao D, Wang Y S, Xue Y Y and Chu C W 2003 *Phys. Rev.* B **67** 134506
[25] Awana V P S, Ichihara S, Nakamura J, Karppinen M and Yamauchi H 2002 *Physica* C **378–381** 249–54
[26] Lal R, Awana V P S, Kishan H, Narlikar A V, Peurla M and Laiho R 2006 *J. Phys.: Condens. Matter* **18** 2563
[27] Cardoso C A, Araujo-Moreira F M, Awana V P S, Takayama-Muromachi E, de Lima O F, Yamauchi H and Karppinen M 2003 *Phys. Rev.* B **67** 02407R
[28] Cardoso C A, Lanfredi A J C, Chiquito A J, Araujo-Moreira F M, Awana V P S, Kishan H and de Lima O F 2005 *Phys. Rev.* B **71** 134509
[29] Awana V P S and Takayama-Muromachii E 2003 *Physica* C **390** 101
[30] Felner I, Schmitt D and Barabara B 1997 *Physica* B **229** 153
[31] Felner I, Hechel D, Rykov A and Raveau B 1994 *Phys. Rev.* B **49** 686
[32] Goodwin T J, Radousky H B and Shelton R N 1993 *Physica* C **204** 212